INTERNATIONAL JOURNAL OF INTEGRATED ENGINEERING
ISSN: 2229-838X e-ISSN: 2600-7916

IJIE

Vol. 16 No. 8 (2024) 236-245
https://publisher.uthm.edu.my/ojs/index.php/ijie

Hydroxyapatite Powders from Chicken Bone Waste: Effect of Low and High-Temperature Calcination

Mohamad Razif Abd Rahman[1], Muhammad Izra Salzamizar Mohd Salehin[1], Mardziah Che Murad[1]*, Mohamed Kamal Abbas[2]

[1] *School of Mechanical Engineering, College of Engineering, Universiti Teknologi MARA, 40450 Shah Alam, Selangor, MALAYSIA*
[2] *Centre for Advanced Materials, Qatar University, P.O. Box 2713, Doha, QATAR*

*Corresponding Author: mardziah31@uitm.edu.my
DOI: https://doi.org/10.30880/ijie.2024.16.08.024

Article Info

Received: 3 July 2024
Accepted: 24 October 2024
Available online: 30 December 2024

Keywords

Beta-tricalcium phosphate, calcination, chicken bone, hydroxyapatite

Abstract

Hydroxyapatite (HA) is a calcium phosphate-based substance that closely mimics the structure and chemical composition of natural bone. Its properties can vary depending on the preparation method and the origin of the precursors. This study aims to thoroughly investigate the properties of HA powders derived from chicken bone waste, obtained at different calcination temperatures. To achieve this, the chicken bones underwent a meticulous cleaning process followed by air drying. Subsequently, the dried bones were finely crushed into smaller pieces and subjected to calcination at 600°C (HA-600) and 1000°C (HA-1000) for comparison. The resulting HA powders were then characterised using a range of analytical techniques, including X-ray diffraction (XRD), Fourier transform infrared spectroscopy (FTIR), and Brunauer-Emmett-Teller (BET) analysis and Field emission scanning electron microscopy (FESEM). The XRD analysis uncovered that HA-600 exhibited a low crystalline HA component, whereas HA-1000 displayed a highly crystalline structure that consists of two distinct phases: HA and beta-tricalcium phosphate (β-TCP). Nonetheless, functional groups such as hydroxyl, phosphate, and carbonate were detected in the FTIR spectra, confirming the formation of HA as the dominant phase in both samples. Additionally, BET analysis disclosed that the average total surface area of the samples was measured as 26.933 cm^3/g and 6.896 cm^3/g for HA-600 and HA-1000, respectively, implying that the powder particles are relatively larger in size for sample calcinated at higher temperature. These findings indicate that subjecting chicken bone-derived HA to high-temperature calcination plays a pivotal role in shaping its properties. This process can be fine-tuned for optimal results, yielding bio-ceramic materials tailored to meet specific requirements in various biomedical applications.

1. Introduction

The last five decades have witnessed a significant surge in research dedicated to enhancing medical materials, especially those employed in skeletal repair and reconstructive surgery [1]. Various materials, including metals, ceramics, composites, and polymers, have been explored for their suitability in supporting complex bone tissue. Among these materials, bio-ceramics stand out as one of the most promising implant options, owing to their

compositional resemblance to bone [2]. Calcium phosphate (CaP)-based bio-ceramics, with their exceptional biocompatibility and chemical stability, have gained widespread acceptance as implant materials [3]. Notably, there are four primary types of CaP: Hydroxyapatite (HA), calcium-deficient hydroxyapatite (CDHA), tricalcium phosphates (TCP), and biphasic calcium phosphate (BCP) [1]. Particularly in disciplines such as orthopedics and dentistry, HA has garnered recognition in the biomedical community due to its remarkable chemical similarity to the mineral phase found in bone tissue. The bone regeneration properties of HA position it as a highly effective synthetic bone substitute, causing its widespread use in the field of regenerative medicine and healthcare [4], [5]. The ongoing global research and development efforts in this domain aim to further expand the applications of HA, contributing to a continuous growth trajectory for the HA market. Projections suggest that the HA market is expected to reach a value of approximately $3 billion by 2023 [6].

Producing HA necessitates a raw material, which can be sourced from either an inorganic or natural origin. Nonetheless, the production of synthetic HA utilizing inorganic precursors carries the risk of generating harmful byproducts, potentially posing environmental hazards [7]. The synthesis of synthetic HA typically entails the utilization of chemicals and elevated temperatures, which may lead to the generation of hazardous waste materials and airborne pollutants. Without appropriate handling, these waste products can exert detrimental effects on the environment, encompassing contamination of water and soil, as well as contributing to air pollution. Natural HA proves to be more accessible and cost-effective when compared to its synthetic counterpart [8]. Among the cost-effective natural biological sources that have undergone extensive scrutiny are eggshells, fish bones, seashells, and various plant materials [9], [10]. It is worth noting that the choice of initial materials used in HA synthesis can influence its structural properties since the behaviour of these precursors undergoes changes during the heating process [1]. In accordance with the findings of Mohd Pu'ad et al. [11], the extraction and recovery of valuable compounds from natural waste materials require specialized techniques to transform these waste resources into useful assets. The transformation process of raw chicken bones into HA powder is shown in Fig. 1.

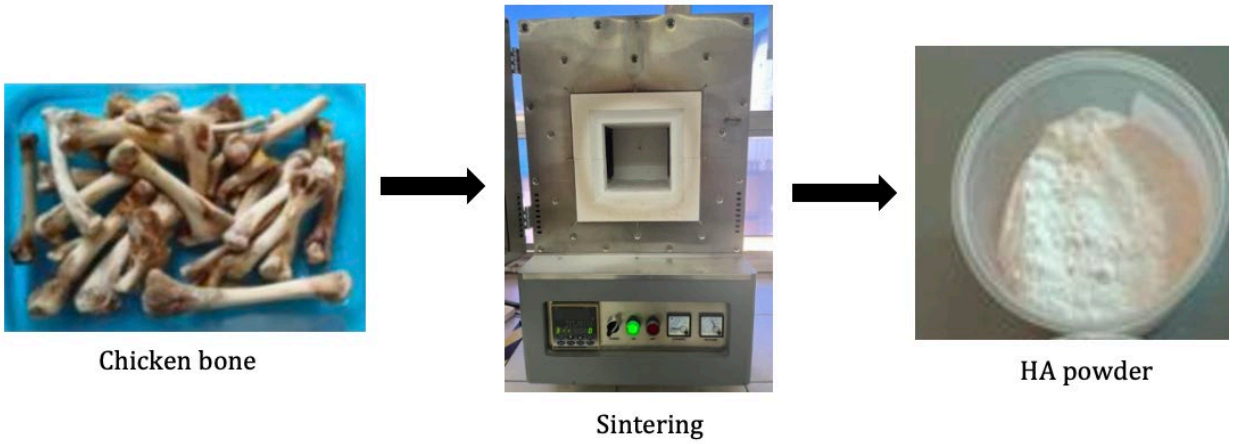

Fig. 1 *Transformation process of raw chicken bones into HA powder*

In this present work, natural HA bio-ceramic derived from chicken bones were studied. The selection of these bones as the natural source is primarily based on their high availability as waste after meat consumption. This characteristic makes them a readily accessible and abundant resource for HA synthesis. One of the core advantages of employing chicken bones lies in their high content of calcium and phosphate, crucial components for HA production. Additionally, chicken bones are abundant and easily procured, presenting a financially efficient and sustainable source of HA. By utilizing chicken bones as a HA source, it concurrently reduces the waste generated by the poultry industry, offering a valuable alternative to conventional waste disposal methods like incineration or landfilling [12]. The utilization of natural sources of calcium and phosphate for HA production not only lessens the environmental impact associated with conventional synthesis methods but also fosters sustainable development [13]. Furthermore, employing chicken bone waste as a raw material for HA synthesis creates a value-added opportunity for the poultry industry, which grapples with significant bio-waste production.

The calcination method is considered an economical and straightforward approach for producing HA powder. In this process, bone particles were placed in an open alumina crucible and heated in a furnace to eliminate organic components, resulting in pure HA. Each sample are typically heated at a predetermined rate and temperature, followed by gradual cooling to room temperature. The properties of HA derived from natural bones are heavily influenced by the chosen synthesis technique, the bone's condition, and the calcination temperature. These attributes encompass characteristics such as particle size distribution and purity. HA can

Int. Journal of Integrated Engineering Vol. 16 No. 8 (2024) p. 236-245

manifest in various microscopic forms, including needles, rods, and spheres, each offering distinct levels of porosity. This porosity plays a crucial role in modulating cell proliferation, adhesion, and the interaction between bone and tissue.

The primary objective of this study is to investigate the effect of low and high calcination temperatures as a means of producing HA from biogenic waste, specifically chicken bone. To achieve this, chicken bone waste was subjected to different thermal treatment at 600°C and 1000°C. The HA powders acquired were subsequently subjected to various characterization techniques to assess their physicochemical properties. Utilizing chicken bone as a resource presents a more economically viable and environmentally friendly alternative to traditional chemical methods. Repurposing bio-wastes to create valuable biomaterials stands as an efficient strategy for both pollution reduction and demonstrating a sustainable approach to solid waste management, all while fostering economic growth.

2. Methodology

2.1 Preparation of Chicken Bone for Thermal Treatment

Firstly, the gathered chicken bones underwent a meticulous cleaning process to remove any remnants of skin and flesh from their surfaces. Subsequently, the bone samples were boiled to eliminate any residual grease. Following this, the bones were left to air-dry for several days until they reached complete dryness. To ensure thorough drying, the samples were then placed in an oven at a temperature of 90°C for 24 hours. After that, the dried bones were pulverized into a powder form through ball milling process, as depicted in Fig. 2. The ball milling process entailed placing bone fragments and grinding balls within a rotating drum. The drum's rotational speed was adjusted to 350 rpm. The ball milling process was carried out for one hour, and this procedure was iterated six times to guarantee comprehensive particle size reduction and uniformity. This iterative process persisted until the desired particle size and uniformity were attained, ultimately yielding finely powdered chicken bones. The chicken bone powder was then carefully transferred to an open alumina crucible with the aid of a spatula before subjected to calcination process.

(a) **(b)**

Fig. 2 *(a) Dried chicken bone; and (b) dried chicken bone crushed into powder form*

2.2 Calcination of the Chicken Bone

Following pre-treatment, the samples were placed in an electric furnace as shown in Fig. 3 and then subjected to calcination under air atmospheric conditions. For comparative purposes, two distinct calcination temperatures (low and high), specifically 600°C and 1000°C, were employed, resulting in the designation of the calcinated samples as HA-600 and HA-1000, respectively. The process entailed a heating rate of 10°C/min with a holding time of 2 hours. Subsequently, the samples produced after the calcination process were finely sieved before undergoing a comprehensive analysis to examine the characteristic properties and formation of HA in both samples.

Fig. 4 illustrates the varying colours exhibited by the final samples due to the different calcination temperatures applied. The transition in colour of the resulting samples from the chicken bone material gradually shifted from a light brownish-yellow shade to a light grey and white, a consequence of the distinct thermal treatment processes. The evolution of colour shades can be attributed to the organic burnout process within the bone samples, as discussed in a previous work by Bee et al. [14]. The HA-600 powders was observed to be greyish in colour, most likely because some ash residue was retained because due to incomplete burning of the organic compound. Fig. 2(a) depicts this grey powder resulting from the calcination process at 600°C.

Conversely, Fig. 2(b) illustrates the HA-1000 sample, characterized by a white hue, indicating the complete elimination of all ash residues from the bone sample at higher temperature.

Fig. 3 *Pulverized chicken powder is placed in the furnace for calcination*

(a) **(b)**

Fig. 4 *Images of (a) HA-600; and (b) HA-1000 calcinated samples*

2.3 Material Characterization Techniques

The analysis of hydroxyapatite (HA) synthesized from chicken bones encompassed a comprehensive suite of analytical methods. These techniques include X-ray diffraction (XRD) analysis, Fourier-transform infrared spectroscopy (FTIR), Brunauer–Emmett–Teller (BET) analysis, and Field-Emission Scanning Electron Microscopy (FESEM). To ascertain the phase composition and crystallinity of the samples, X-ray diffraction (XRD) analysis was performed using a Rigaku Model Ultima IV diffractometer. The XRD spectra were recorded across a 2θ angle range of 10° to 90°, employing CuKα radiation at 40 kV and 40 mA. Peak comparison was made with the International Centre for Diffraction Data (ICDD) for HA and β-TCP, with reference codes 01-082-2956 and 01-070-2065, respectively. On the other hand, for the investigation of functional groups and chemical bonds, FTIR analysis was conducted on HA-600 and HA-1000 samples using a PerkinElmer Spectrum One spectrometer, spanning a range of 500 cm^{-1} to 4000 cm^{-1}. The determination of specific surface area, total pore volume, and average pore diameter of the powders was accomplished through BET analysis, utilizing a Micrometric 3Flex 3500 instrument. Nitrogen gas adsorption facilitated the calculation of specific surface area, pore size distribution, and pore volume. Morphological examination of the particles involved the use of FESEM, specifically a Jeol JSM-7600F instrument, which provided high-resolution imaging and detailed surface morphology analysis. A flowchart that describes the processes involved in the development of HA powder from chicken bones and its characterization is presented in Fig. 5.

Int. Journal of Integrated Engineering Vol. 16 No. 8 (2024) p. 236-245

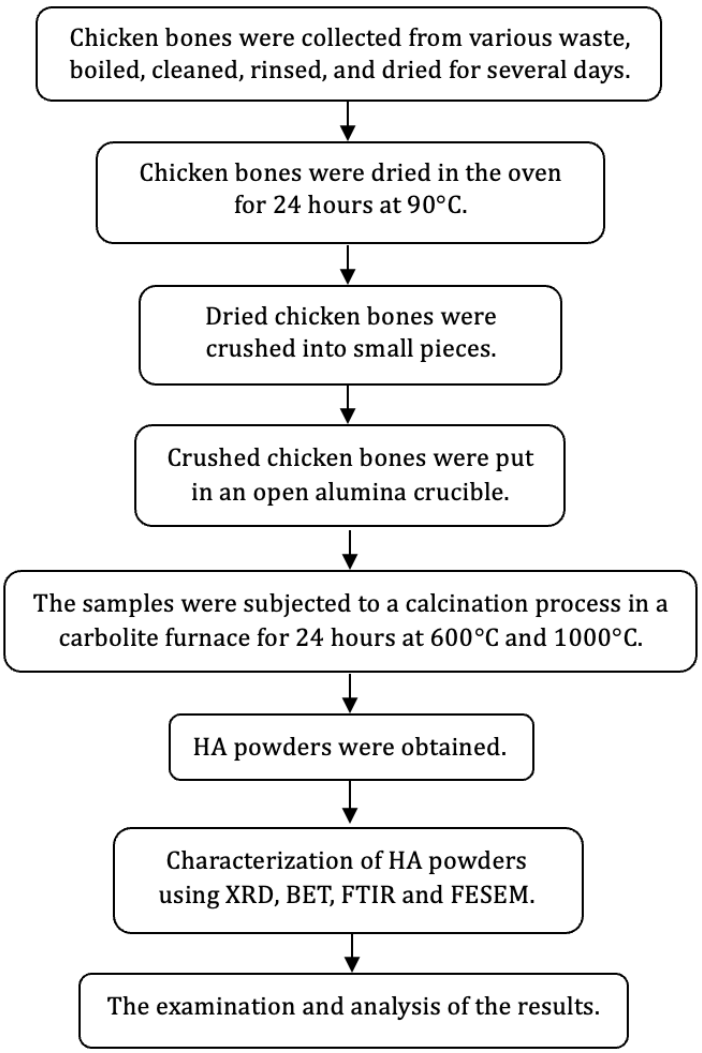

Fig. 5 *Flowchart that describes the process of obtaining HA powders from chicken bones, followed by their characterizations and analyses*

3. Results

3.1 XRD Analysis

The X-ray Diffraction (XRD) analysis of the HA-600 and HA-1000 samples are shown in Fig. 6(a) and Fig. 6(b), respectively. Within the XRD spectrum of HA-600, the most prominent peaks were detected at a 2θ angle of 31.9° and 32.2°. The presence of these peak conclusively indicated the prevalence of the HA phase within the sample [15], but at a slightly lower crystallinity. Similarly, the XRD spectrum of HA-1000 unveiled striking peaks at a 2θ angle of 31.9°, 32.1° and 32.9° with much higher intensity, unequivocally affirmed the conversion of the raw material into crystalline HA. These peak served as compelling evidence for the presence of HA as a dominant phase within the HA-1000 sample. However, secondary phase of β-TCP was also detected based on the presence of its peak at approximately 30.7°, confirming the formation of biphasic calcium mixture (HA+β-TCP) in the HA-1000 sample. Phase content for both samples is displayed in Table 1.

Table 1 *Phase content for HA-600 and HA-1000 samples*

Sample	HA (%)	β–TCP (%)
HA-600	100	0
HA-1000	89.3	10.7

The XRD analysis of both HA-600 and HA-1000 samples delivered invaluable insights into their crystallographic properties, reaffirming the formation of HA in both instances. Notably, the XRD analysis of HA-1000 showcased superior crystallinity compared to HA-600. This superiority was evidenced by the heightened

intensity of the characteristic peak at a 2θ angle and the sharper peak profile. This enhanced crystallinity within HA-1000 can be attributed to improved crystal growth and a reduced amorphous content, indicative of a more well-defined and ordered crystal lattice structure. The heightened crystallinity observed in HA-1000 accentuates its superior stability and potential for enhanced material properties.

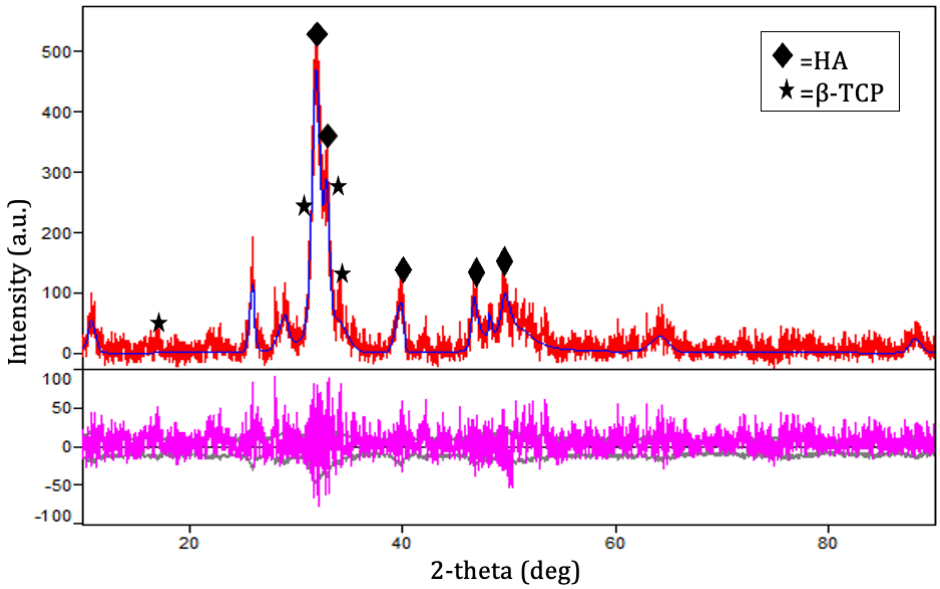

(a)

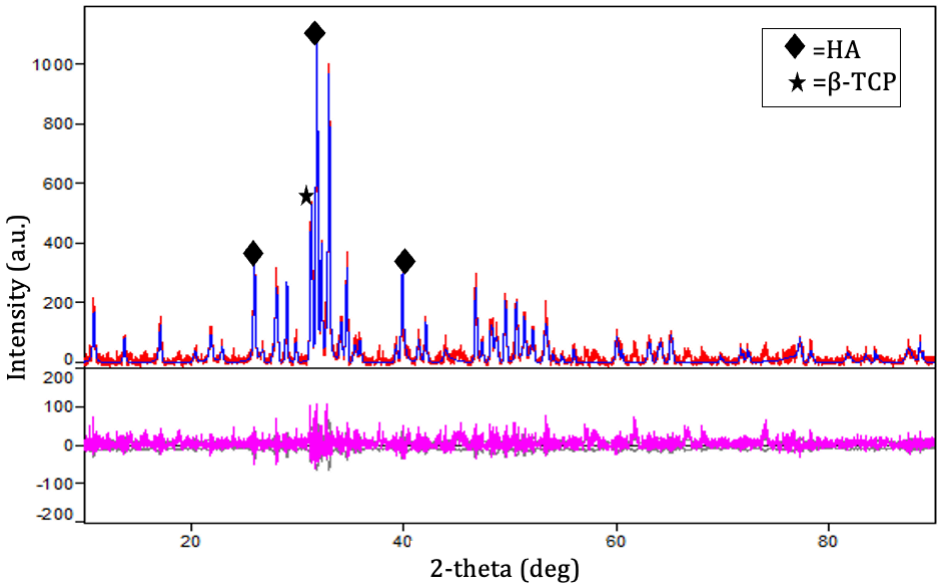

(b)

Fig. 6 *XRD patterns of (a) HA-600; and (b) HA-1000 samples*

3.2 FTIR Analysis

Functional group detection for phosphate, carbonate, and hydroxyl in HA can be greatly aided by the FTIR spectral analysis. The FTIR graph for HA were divided into several regions, each corresponding to a different functional group or type of chemical bonding. The phosphate region (850-1200 cm^{-1}) shows several peaks that correspond to the stretching and bending vibrations of the phosphate groups in HA. The hydroxyl region (3000-3800 cm^{-1}) shows a broad absorption band that corresponds to the stretching vibration of the hydroxyl (OH^-) groups in HA.

Fig. 7 and Fig. 8 show the FTIR spectrum of HA-600 and HA-1000, respectively, which shows several characteristic peaks that correspond to the different functional groups in the HA structure. For example, the phosphate (PO_4^{3-}) group produces strong absorption bands between 850 and 1200 cm^{-1} for both graphs, while

Int. Journal of Integrated Engineering Vol. 16 No. 8 (2024) p. 236-245

the OH^- group appears as a broad absorption band around 3400 cm^{-1}. At approximately 3572 cm^{-1}, similar OH band with the lowest intensity can be observed, but it corresponds to the stretching mode of the OH structural group [8]. Both HA-600 and HA-1000 samples displayed the four characteristic bands for PO groups at 1049-1092 cm^{-1}, due to the symmetrical O-P-O bending (ν_3), the band at 962 cm^{-1} is due to the symmetrical P-O stretching (ν_1), and the band at 569-570 cm^{-1}, 601–603 cm^{-1} is due to the anti-symmetric O-P-O bending (ν_4), and finally a P-O stretching (ν_2) band can be detected at the range of 470-472 cm^{-1} [16]. It should be highlighted that, the presence of these bands are often associated with HA structure characteristics. On the other hand, the manifestation of CO band can only be seen in the HA-1000 (at approximately 850–900 cm^{-1}), probably because it contains biphasic mixture, unlike HA-600. The HA-1000 sample not only comprises the β-TCP phase but is also notably more crystalline compared to HA-600, a fact corroborated by the XRD pattern shown in Fig. 6. The FTIR result of these calcinated samples is in good agreement with the previous report for natural HA extracted from the fish scale [17].

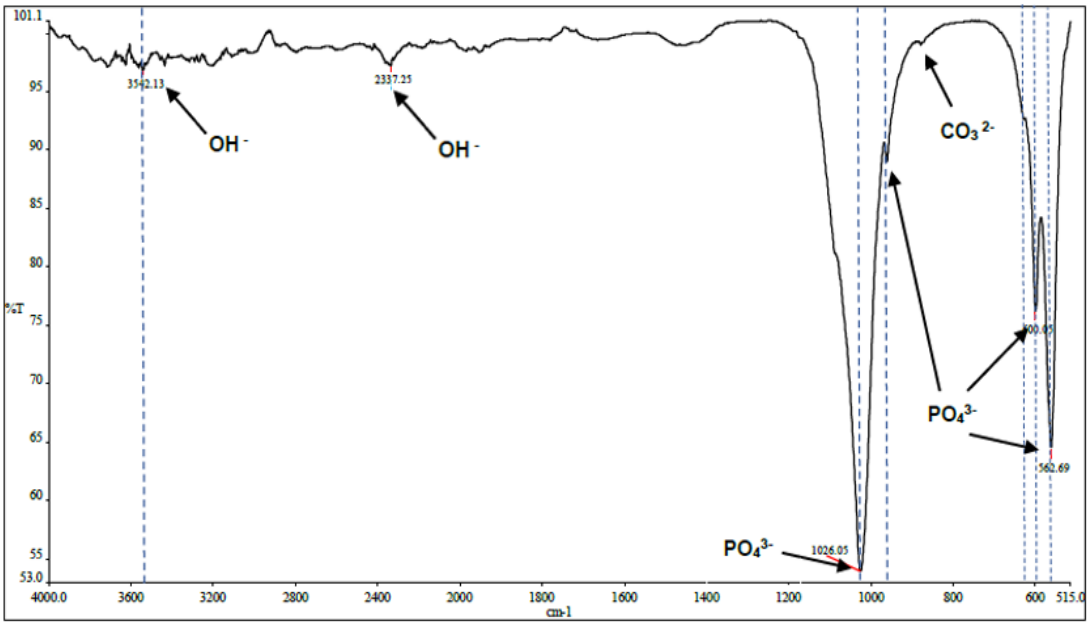

Fig. 7 *FTIR spectra of HA-600*

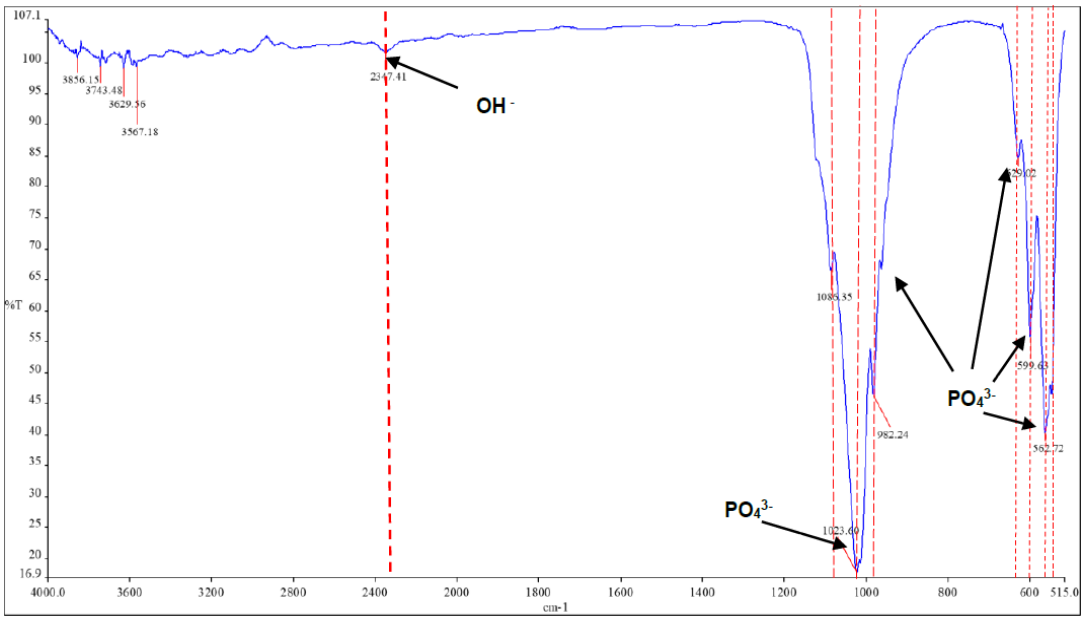

Fig. 8 *FTIR spectra of HA-1000*

3.3 BET Analysis

Table 2 presents the results obtained from the BET analysis, offering valuable insights into the surface attributes of the generated HA powders such as specific surface area (S_{BET}), the total pore volume (V_T), and the average pore diameter (D_{avg}). The HA-600 sample displayed notable distinctions compared to HA-1000 sample. Upon analysing the BET results, it becomes evident that the surface area of the HA-600 sample surpasses that of HA-1000, recording values of 26.933 m^2/g and 6.896 m^2/g, respectively. This disparity implies that the powder particles in HA-600 sample were much smaller than the particles in HA-1000. This observation aligns with the expected behavior, as higher calcination temperatures tend to promote particle growth. Likewise, the total pore volume within the HA-600 sample significantly outpaces that of HA-1000, with respective values of 0.215 cm^3/g and 0.008 cm^3/g. Moreover, the analysis also unveiled the average pore diameter (D_{avg}) for HA-600 sample exhibited a larger average pore size, measuring 32.563 nm, whereas the HA-1000 sample displayed a much smaller value of 4.952 nm.

Table 2 *BET surface analyzer data for HA-600 and HA-1000 samples*

Sample	Surface area, S_{BET} (m^2/g)	Total pre volume, V_T (cm^3/g)	Average pore diameter, D_{avg} (nm)
HA-600	26.933	0.215	32.563
HA-1000	6.896	0.008	4.952

3.4 FESEM Morphological Observation

Fig. 9 presents the FESEM image of HA-1000, in which the particle size was found to be in the range of 10 to 50 µm. The observed phenomenon of particle agglomeration in the powders is mainly attributed to a combination of high collective energy among small particles and van der Waals attraction [18]. Subsequent to the removal of organic elements from the chicken bone, the morphological examination of samples resulting from thermal calcination at 1000°C unveiled a porous network. As elucidated in a study by Ramesh and colleagues [19], the appearance of this porous network within the matrix could be attributed to the breakdown of organic components within the chicken bone during the thermal treatment process.

The FESEM images also distinctly illustrate that HA-1000 particles possess a structure akin to flakes and has a coarse surface. On the other hand, the morphology of HA-600 was not observed under FESEM because it did not meet the criteria for classification as bio-ceramic material. The HA-600 powder displayed a greyish hue, possibly attributed to the presence of ash residue resulting from incomplete organic incineration. It is important to highlight that the US Food and Drug Administration (FDA) mandates that HA powder must exhibit a pristine, white coloration [20].

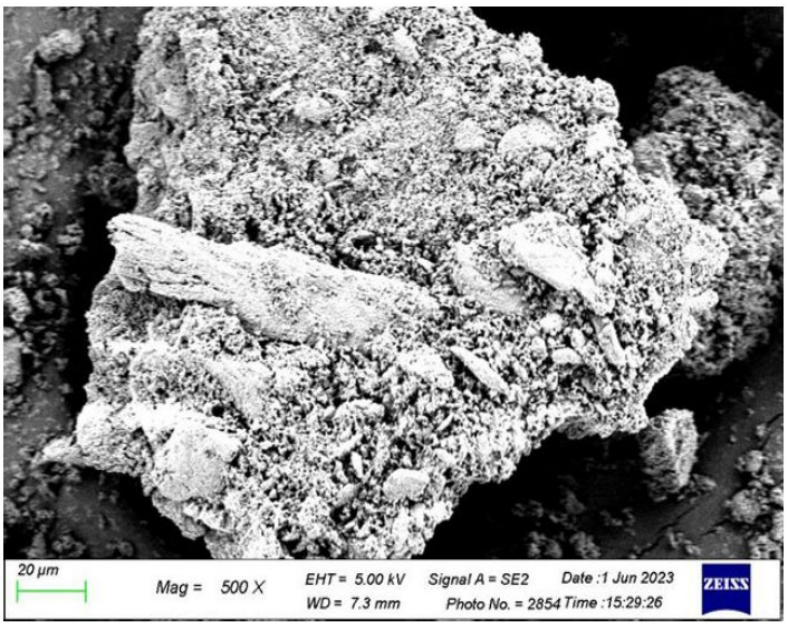

Fig. 9 *SEM micrograph of HA-1000 sample*

4. Conclusions

In this present study, we successfully synthesized HA powders at two different temperatures, 600°C and 1000°C, by utilizing chicken bone waste via the direct calcination method. XRD analysis carried out on both HA-600 and HA-1000 samples confirmed the establishment of HA as the main phase. XRD peaks for HA-600 were observed to be broader and less intense, implying that it had not yet achieved a fully crystalline state. In contrast, the XRD patterns for HA-1000 indicate a well-defined crystalline structure of HA and β-TCP, confirming the formation of a biphasic calcium mixture of ceramic powders. This investigation also highlighted the influence of calcination temperature on crystallinity and phase composition, with higher temperatures favouring β-TCP formation. A noteworthy distinction observed in the FTIR spectra was the absence of the carbonate group in the HA-1000 sample, most likely due to the presence of secondary phase, β-TCP as well as its improved level of crystallinity. FESEM micrograph of HA-1000 exhibits flake-like powder shape with coarse surface particles that is highly agglomerated. The results from this study indicate that the formation of high crystalline HA powders can be attained at high temperature calcination (1000°C) but not at lower temperature (600°C). The increased level of crystallinity observed in HA-1000 highlights its superior stability as a more promising bio-ceramic material. In conclusion, the utilization of chicken bones for HA synthesis represents a promising avenue for the creation of cost-effective, biocompatible biomaterials. This approach not only offers economic advantages but also aligns with sustainable and environmentally friendly practices.

Acknowledgement

This research was funded by a grant from Ministry of Higher Education of Malaysia (FRGS Grant No: FRGS/1/2023/TK09/UITM/02/2). The authors would also like to thank College of Engineering, Universiti Teknologi MARA (UiTM) for the technical and financial supports.

Conflict of Interest

Authors declare that there is no conflict of interests regarding the publication of the paper.

Author Contribution

The authors confirm contribution to the paper as follows: ***study conception and design:*** *Mardziah Che Murad;* ***data collection:*** *Mohamad Razif Abd Rahman;* ***analysis and interpretation of results:*** *Mohamad Razif Abd Rahman, Muhammad Izra Salzamizar Mohd Salehin, Mardziah Che Murad;* ***draft manuscript preparation:*** *Mohamad Razif Abd Rahman, Mardziah Che Murad, Mohamed Kamal Abbas. All authors reviewed the results and approved the final version of the manuscript.*

References

[1] Goh, K. W., Wong, Y. H., Ramesh, S., Chandran, H., Krishnasamy, S., Ramesh, S., Sidhu, A. & Teng, W. D. (2021). Effect of pH on the properties of eggshell-derived hydroxyapatite bioceramic synthesized by wet chemical method assisted by microwave irradiation, Ceramics International, 47, 8879–8887. https://doi.org/10.1016/j.ceramint.2020.12.009

[2] Akram, M. & Ahmed, R. (2014). Extracting hydroxyapatite and its precursors from natural resources. Journal of Materials Science, 49, 1461–1475. https://doi.org/10.1007/s10853-013-7864-x

[3] Song, J., Liu, Y., Zhang, Y. & Jiao, L. (2011). Mechanical properties of hydroxyapatite ceramics sintered from powders with different morphologies. Materials Science and Engineering: A, 528, 5421–5427. https://doi.org/10.1016/j.msea.2011.03.078

[4] Kalbarczyk, M. & Szcześ, A. (2021). Potential biomedical application of calcium phosphates obtained using eggshells as a biosource of calcium at different initial pH values. Ceramics International, 47, 33687–33696. https://doi.org/10.1016/j.ceramint.2021.08.278

[5] Kılınç, A. C., Köktaş, S. & Göktaş, A. A. (2021). Characterization of eggshell-derived hydroxyapatite on Ti6Al4V metal substrate coated by sol–gel method. Journal of the Australian Ceramic Society, 57, 47–53. https://doi.org/10.1007/s41779-020-00511-y

[6] Maidaniuc, A., Miculescu, F., Ciocoiu, C., Butte, T. M., Pauk, I., Stan, G. E., Voicu, I. & Ciocan, L. T. (2020). Effect of the processing parameters on surface, physico-chemical and mechanical features of bioceramics synthesized from abundant carp fish bones. Ceramics International, 46, 10159–10171. https://doi.org/10.1016/j.ceramint.2020.01.007

[7] Qin, D., Bi, S., You, X., Wang, M., Cong, X., Yuan, C., Yu, M., Cheng, X. & Chen, X. G. (2022). Development and application of fish scale wastes as versatile natural biomaterials. Chemical Engineering Journal, 428, 131102. https://doi.org/10.1016/j.cej.2021.131102

[8] Mardziah, C. M., Ramesh, S., Tan, C. Y., Chandran, H., Sidhu, A., Krishnasamy, S. & Purbolaksono, J. (2021). Zinc-substituted hydroxyapatite produced from calcium precursor derived from eggshells, Ceramics International, 47, 33010–33019. https://doi.org/10.1016/j.ceramint.2021.08.201
[9] Nga, N. K., Thuy Chau, N. T. & Viet, P. H. (2018). Facile synthesis of hydroxyapatite nanoparticles mimicking biological apatite from eggshells for bone-tissue engineering. Colloids and Surfaces B: Biointerfaces, 172, 769–778. https://doi.org/10.1016/j.colsurfb.2018.09.039
[10] Thirukumaran, R., Anu Priya, V. K., Krishnamoorthy, S., Ramakrishnan, P., Moses, J. A. & Anandharamakrishnan, C. (2022). Resource recovery from fish waste: Prospects and the usage of intensified extraction technologies. Chemosphere, 299, 134361. https://doi.org/10.1016/j.chemosphere. 2022.134361
[11] Mohd Pu'ad, N. A. S., Abdul Haq, R. H., Mohd Noh, H., Abdullah, H. Z., Idris, M. I. & Lee, T. C. (2020). Synthesis method of hydroxyapatite: A review. Materials Today: Proceedings, 29, 233–239. https://doi.org/10.1016/ j.matpr.2020.05.536
[12] Ghosh, S. & Pramanik, K. (2023). Unveiling the secrets of food waste derived biomaterials in remediation of environmental pollutants – A review. Bioresource Technology Reports, 22, 101469. https://doi.org/ 10.1016/j.biteb.2023.101469
[13] Borciani, G., Fischetti, T., Ciapetti, G., Montesissa, M., Baldini, N. & Graziani, G. (2023). Marine biological waste as a source of hydroxyapatite for bone tissue engineering applications. Ceramics International, 49, 1572–1584. https://doi.org/10.1016/j.ceramint.2022.10.341
[14] Bee, S. & Hamid, Z. A. A. (2020). Hydroxyapatite derived from food industry bio-wastes: Syntheses, properties and its potential multifunctional applications, Ceramics International, 46, 17149–17175. https://doi.org/10.1016/j.ceramint.2020.04.103
[15] Mardziah, C. M., Abdul Wahid, M. F., Hyie, K. M., Masdek, N. R. N. & Salleh, Z. (2017). Effect of sintering temperature on zinc substituted calcium phosphate ceramics. Materials Science Forum, 890, 209–212. https://doi.org/10.4028/www.scientific.net/ MSF.890.209
[16] Forero-Sossa, P. A., Olvera-Alvarez, I. U., Salazar-Martinez, J. D., Espinosa-Arbelaez, D. G., Segura-Giraldo, B. & Giraldo-Betancur, A. L. (2021). Biogenic hydroxyapatite powders: Effects of source and processing methodologies on physicochemical properties and bioactive response. Materials Characterization, 173, 110950. https://doi.org/10.1016/j.matchar.2021.110950
[17] Deb, P., Barua, E., Deoghare, A. B. & Das Lala, S. (2019). Development of bone scaffold using Puntius conchonius fish scale derived hydroxyapatite: Physico-mechanical and bioactivity evaluations. Ceramics International, 45, 10004–10012. https://doi.org/10.1016/j.ceramint.2019.02.044
[18] Luo, Y., Zhao, R., & Pendry, J. B. (2014). van der Waals interactions at the nanoscale: The effects of nonlocality. Proceedings of the National Academy of Sciences, 111, 18422-18427. https://doi.org/ 10.1073/pnas.1420551111
[19] Ramesh, S., Loo, Z. Z., Tan, C. Y., Kelvin Chew, W. J., Ching, Y. C., Tarlochan, F., Chandran, H., Krishnasamy, S., Bang, L. T. & Sarhan, A. A. D. (2018). Characterization of biogenic hydroxyapatite derived from animal bones for biomedical applications. Ceramics International, 44, 10525–10530. https://doi.org/10.1016/ j.ceramint. 2018.03.072
[20] Salma-Ancane, K., Stipniece, L. and Irbe, Z. (2016). Effect of biogenic and synthetic starting materials on the structure of hydroxyapatite bioceramics. Ceramics International, 42, 9504–9510. https://doi.org/10.1016/ j.ceramint.2016.03.028